EphrinB reverse signaling contributes to endothelial and mural cell assembly into vascular structures

Ombretta Salvucci,[1] Dragan Maric,[2] Matina Economopoulou,[1] Shuhei Sakakibara,[1] Simone Merlin,[3] Antonia Follenzi,[3,4] and Giovanna Tosato[1]

[1]Laboratory of Cellular Oncology, Center for Cancer Research, National Cancer Institute, and [2]Laboratory of Neurophysiology, National Institute of Neurological Disorders and Stroke, National Institutes of Health, Bethesda MD; [3]Department of Medical Sciences, University of Piemonte Orientale School of Medicine, Novara, Italy; and [4]Department of Pathology, Marion Bessin Liver Research Center, Albert Einstein College of Medicine, New York, NY

EphrinB transmembrane ligands and their cognate EphB receptor tyrosine kinases regulate vascular development through bidirectional cell-to-cell signaling, but little is known about the role of EphrinB during postnatal vascular remodeling. We report that EphrinB is a critical mediator of postnatal pericyte-to-endothelial cell assembly into vascular structures. This function is dependent upon extracellular matrix-supported cell-to-cell contact, engagement of EphrinB by EphB receptors expressed on another cell, and Src-dependent phosphorylation of the intracytoplasmic domain of EphrinB. Phosphorylated EphrinB marks angiogenic blood vessels in the developing and hypoxic retina, the wounded skin, and tumor tissue, and is detected at contact points between endothelial cells and pericytes. Furthermore, inhibition of EphrinB activity prevents proper assembly of pericytes and endothelial cells into vascular structures. These results reveal a role for EphrinB signaling in orchestrating pericyte/endothelial cell assembly, and suggest that therapeutic targeting of EphrinB may prove useful for disrupting angiogenesis when it contributes to disease. (Blood. 2009;114:1707-1716)

Introduction

Blood vessels are composed of endothelial cells that form the inner lining of vessels and pericytes, also known as mural cells, that envelope the endothelium. Pericytes are embedded into the vascular basement membrane and make direct contact with endothelial cells through extensions that reach deeply into the endothelial cells, without an intervening basal membrane.[1,2] Endothelial cells are better characterized, but pericytes are emerging as critical regulators of vascular function because they are thought to stabilize the vessel wall and to regulate endothelial cell survival, growth, maturation, and permeability.[2] Pericytes have multilineage progenitor potential and are developmentally close to mesenchymal stem cells (MSCs).[3]

Genetic mouse models have implicated several receptor-ligand systems as mediators of endothelial-pericyte interactions, including Ang-1/Tie2, transforming growth factor-β and its receptors, platelet-derived growth factor (PDGF)/PDGF receptor-1, the sphingosine-1-phosphate (S1P)/$S1P_1$, and Dll4/Notch.[2] The family of EphB (erythropoietin-producing hepatoma) receptors tyrosine kinases and their surface-bound EphrinB (erythropoietin-producing hepatoma interactor B) ligands have recently emerged as critical regulators of cardiovascular development and pathologic angiogenesis, modulating both endothelial cells and pericyte function.[4] Upon cell-to-cell contact, EphrinB ligands both activate the cognate EphB receptors (forward signaling) and undergo phosphorylation at the C terminus initiating signaling (reverse signaling).[5,6] Genetic experiments have shown that the global knockout of EphB4, EphrinB2, or the endothelial-specific inactivation of EphrinB2 produced a very similar phenotype of embryonic death with prominent remodeling defects of the vascular system.[7-9] The role of EphrinB2 reverse signaling in vascular development is controversial. Targeted removal of the EphrinB2 carboxy-terminal cytoplasmic tail was shown to disrupt vascular development and result in embryonic lethality similar to the null EphrinB2 mutation.[10] Other studies found that EphrinB2 reverse signaling is not required during vascular development, but is necessary for maturation of the cardiac valves.[11] Knock-in mice expressing mutant EphrinB2 in which the conserved tyrosine residues were substituted or lacked PDZ interaction site had no appreciable vascular defects.[12] More recently, the selective inactivation of EphrinB2 in mural cells caused perinatal death, and the mutant mice displayed hemorrhaging and edema in various tissues,[13] which was attributed to the failure of mural cells to migrate, attach, and properly cover the blood vessel endothelium.

Despite genetic evidence for their critical role during vascular development, the role of EphrinB2 and its Eph receptors in postnatal vascular remodeling is less clear. EphrinB2 is expressed in the endothelium and mural cells of adult arteries, arterioles, and capillaries in many tissues.[14,15] Adult endothelial cells constitutively express EphB2 and EphB4.[16] Vascular EphrinB2 levels increase during angiogenesis[14] and in response to cyclic stretch.[17] Functional studies in vitro have produced conflicting results. In some systems, activation of EphB receptors and EphrinB ligands promoted endothelial cell sprouting, migration, and assembly into cordlike structures,[18-20] and the blockade of EphB/EphrinB interactions reduced endothelial cell assembly into cordlike structures.[16] In other systems, activation of EphB4 reduced endothelial cell migration, adhesion, and proliferation,[21,22] and the activation of EphB receptors reduced smooth muscle cell migration.[17]

Submitted November 28, 2008; accepted April 22, 2009. Prepublished online as *Blood* First Edition paper, May 1, 2009; DOI 10.1182/blood-2008-12-192294.

The online version of this article contains a data supplement.

The publication costs of this article were defrayed in part by page charge payment. Therefore, and solely to indicate this fact, this article is hereby marked "advertisement" in accordance with 18 USC section 1734.

In this study, we have explored the contribution of EphrinB to the assembly of endothelial cells and pericytes during postnatal angiogenic remodeling.

Methods

Cells and reagents

Endothelial cells from the human umbilical vein (HUVEC) were propagated through passage 6.[23] Human bone marrow–derived MSC (BM-MSC; Cambrex BioScience) were propagated in Dulbecco modified Eagle medium, low glucose (Invitrogen). MSC tested positive for CD29, CD44, CD90, CD105, and CD166; negative for CD13, CD31, CD34, CD45, CD117, Flk1, Flt1, and CXC chemokine receptor (CXCR)4; and differentiated into adipocytes and bone cells by standard methods. Recombinant mouse EphrinB2-Fc and EphB4-Fc, recombinant human immunoglobulin (Ig)G1-Fc, goat anti–mouse EphrinB2 (specificity validated by immunoblotting cell lysates of MSC overexpressing EphrinB2), EphB2 and EphB4, and sheep anti–human CD31/platelet endothelial cell adhesion molecule-1 (PECAM-1) antibodies were from R&D Systems. Rabbit antibodies to phospho-signal transducer and activator of transcription (STAT)3 (Tyr^{705}) and to phospho-EphrinB ($Tyr^{324/329}$), and mouse monoclonal antibody L4A1 to Src were from Cell Signaling Technology; goat anti–actin antibody was from Santa Cruz Biotechnology; rabbit anti–NG2 chondroitin sulfate proteoglycan polyclonal antibody was from Chemicon International; mouse monoclonal antibodies to STAT3, human CD31/PECAM-1 (fluorescein isothiocyanate [FITC] labeled), and human CD90 (phycoerythrin [PE] labeled) were from BD Pharmingen; Alexa Fluor 488 goat anti–rabbit IgG and Alexa Fluor 546 donkey anti–sheep IgG were from Molecular Probes/Invitrogen; and horseradish peroxidase–conjugated donkey anti–mouse and anti–rabbit IgG were from Calbiochem. CellTrace CFSE (5-(and 6-)carboxyfluorescein diacetate succinimidyl ester) Cell Proliferation Kit (Molecular Probes) and PKH26 red fluorescent cell linker kit were from Sigma-Aldrich. The SNEW peptide (SNEWIQPRLPQH), the scrambled peptide SCR-EPQ (EPQNHSWPIRQL), the TNYL-RAW peptide (YNYLF-SPNGPIARAW), and the scrambled peptide SCR-WTL (WTLAIFARNYN-GPSP) were from Sigma Genosys. The inhibitors 4-amino-5-(4-chlorophenyl)-7-(*t*-butyl)pyrazolo[3,4-*d*]pyrimidine (PP2) and AG490 were from Calbiochem.

EphrinB2, Src, and Janus kinase 2 silencing and green fluorescent protein expression

ON-TARGETplus small interfering RNAs (siRNAs) for human EphrinB2, Src, and Janus kinase 2 (Jak2) and Risc-free control siRNA were purchased from Dharmacon. siRNA (100 nM) was transfected into cells using Oligofectamine reagent (Invitrogen). Third-generation lentivirus (vesicular stomatitis virus glycoprotein [VSV-g]–pseudotyped HIV-1 based) expressing short hairpin RNA (shRNA) constructs against human EphrinB2 and control lentivirus were generated by cotransfection of 293T cells.[24] The 293T cells were cotransfected with 4 plasmids, as follows: a cytomegalovirus (CMV) promoter-driven packaging construct expressing the *gag* and *pol* genes, a Rous sarcoma virus promoter-driven construct expressing *rev*, a CMV promoter-driven construct expressing the VSV-g envelope, and a self-inactivating transfer construct from MISSION shRNA (Sigma NM-004093) containing the expression cassette driven by the human U6 promoter containing a shRNA against EphrinB2 and a second cassette driven by the human phosphor glycerate kinase promoter in which the Puromycin gene was removed by the restriction digestion with the *Bam*HI and *Kpn*I enzymes and enhanced green fluorescent protein (GFP) was inserted as a marker gene. Control lentivirus was generated by transfecting 293T cells with the packaging, Rev-expressing, Env-expressing, and basal transfer construct, without shRNA sequence. Virus-containing supernatant was collected 24 hours and 48 hours after transfection, concentrated, titrated ($1\text{-}2 \times 10^9$ transducing U/mL), and frozen (−80°C) until use. Five different shRNA-LV constructs (TRCN000005842 nos. 3, 4, 5, 6, and 7) were tested in vitro for EphrinB2 silencing in target cells; the most effective (TRCN0000058424) was selected for use. The previously described GFP lentivirus vector was used for cell labeling.[25] HUVEC and MSC were exposed to virus in complete culture medium for 18 hours. Cell transduction efficiency was evaluated by flow cytometric analysis of GFP expression; EphrinB2 silencing was evaluated by real-time reverse transcription–polymerase chain reaction (RT-PCR). pEYFP-ephrinB2^{WT} and pEYFP-EphrinB2^{5Y} were a gift from T. Makinen[12] (Lymphatic Development Laboratory, Cancer Research UK, London Research Institute, London, United Kingdom). pEYFP-EphrinB2^{5Y} codes for a fusion protein of rodent phlorizin hydrolase-derived signal peptide (MELFWSIVFTVLLSF-SCRGSDW), yellow fluorescent protein (EYFP), and influenza virus hemagglutinin (YPYDVPDYA)-tagged mouse ephrinB2 (aa 27-337). For construction of pEYFP-EphrinB2^{5F}, in which tyrosine residues at 307, 314, 319, 333, and 334 are substituted with phenylalanine, pEYFP-EphrinB2^{5Y} (Erratum Genes & Development 20:1829, 2006) was modified by PCR-based techniques. Correct plasmid construction was confirmed by DNA sequencing (DNA Minicore Facility, National Cancer Institute, National Institutes of Health, Bethesda, MD). Expression of pEYFP-ephrinB2^{WT} and pEYFP-EphrinB2^{5Y} in HUVEC and MSC was achieved with Amaxa nucleofector system with specific cell-type optimization (Amaxa Biosystems).

Real-time RT-PCR

RNA was extracted using TRI Reagent (Molecular Research Center); cDNA was synthesized from 1 μg total RNA (High Capacity cDNA Reverse Transcription Kit; Applied Biosystems, Foster City, CA). EphrinB2 mRNA was measured by real-time PCR (Assay-on-Demand Taqman Gene expression probes; Applied Biosystems) with 1 μL cDNA with ABI Prism 7900 sequence detection system (Applied Biosystems); mRNA levels were expressed as relative units.

Western blotting

Cell lysates for phosphorylated proteins were prepared in sodium dodecyl sulfate (SDS) lysis buffer (50 mM Tris [pH 7.4], 150 mM NaCl, and 1% SDS) with protease inhibitor mixture set III (Calbiochem), 50 mM NaF, and 1 mM sodium orthovanadate. Other lysates were prepared in tricine-SDS sample buffer (Novex). Protein extracts resolved in NuPage 4%-12% bis-Tris gels (Invitrogen) or 10%-20% polyacrylamide gels (Novex) were transferred to protran BA83 cellulosenitrate membranes (Whatman) and immunostained, as described.[16] Membranes were stripped and restained. Bands were measured by NIH Image software.

Flow cytometry

HUVEC and BM-MSC were detached with 5 mM EDTA (ethylenediaminetetraacetic acid) in phosphate-buffered saline (PBS) at 4°C, washed (MEDIUM199, 1% fetal bovine serum, 10 mM HEPES (N-2-hydroxyethylpiperazine-N′-2-ethanesulfonic acid), and stained with anti–human CD31 FITC and anti–human CD90-PE (BD Biosciences) at 4°C. Cells were suspended (250 μL of Citofix/Cytoperm solution; 20 minutes, 4°C; BD Biosciences), washed, blocked (0.5% bovine serum albumin [BSA] in PBS, 10 minutes), and stained for intracellular phospho-EphrinB (rabbit anti–phospho-EphrinB/$Tyr^{324/329}$; 1/100 dilution; Cell Signaling Technology), followed by staining with goat anti–rabbit IgG PE-Cy5 (Caltag Laboratories). Data were collected using a FACSCalibur cytofluorometer (BD Biosciences).

Immunohistochemistry

For retinal whole mounts, eyes were fixed in 2% paraformaldehyde for 30 minutes; intact retinas were removed. After rinsing (twice PBS for 20 minutes), blocking (PBS with 5% mouse serum, 0.2% BSA, and 0.3% Triton X-100 for 30 minutes), and washing, retinas were immunostained. Other tissues were fixed (cold 4% paraformaldehyde in PBS), soaked in 15% and 30% sucrose, embedded in OCT, and processed for histology. Sections were stained with hematoxylin and eosin (H&E) or immunostained with rat anti–mouse CD31/PECAM monoclonal antibody (BD Pharmingen), followed by Alexa Fluor 647–conjugated goat anti–rat IgG

(Molecular Probes); rabbit IgG anti–human phospho-EphrinB (Tyr$^{324/329}$; Cell Signaling Technology), followed by Alexa Fluor 488 goat anti–rabbit IgG antibody (Molecular Probes); rabbit IgG anti–NG2 polyclonal antibody (Chemicon International) conjugated with Alexa Fluor 546 using a Zenon rabbit IgG labeling kit (Molecular Probes); and goat anti–mouse EphrinB2 (R&D Systems), followed by Alexa Fluor 594 donkey anti–goat IgG.

Laser confocal microscopy

Confocal images were acquired with Zeiss AIM software on a Zeiss LSM 510 confocal system (Carl Zeiss) with a Zeiss Axiovert 100 M inverted microscope equipped with a 50 mW argon ultraviolet laser tuned to 364 nm, a 25 mW Argon visible laser tuned to 488 nm, a 1 mW HeNe laser tuned to 543 nm, and a 5 mW HeNe laser tuned to 633 nm. A 40×/1.3 numeric aperture (NA) Plan-Neofluar and a 63×/1.4 NA Plan-Neofluar oil-immersion objective were used at various digital zoom settings. Emission signals were collected with a BP 385-470, BP 505-550, LP 560 filter or LP 650 filters, using individual Z-stacks consisting of 18-20 slices at 1-mm intervals. Z-stacks were used with Bitplane Imaris software (v6.0) for surface rendering.

In vitro Matrigel assay

Cord formation assay was carried out as described.[26] Endothelial cells (HUVEC, 4×10^4; BM-MSC, 2×10^4) and MSC were incubated ($4\text{-}5 \times 10^4$; 37°C, 18 hours) individually or together onto 24-well tissue-culture plates precoated (200-300 μL Matrigel; Collaborative; BD Pharmingen) in HUVEC culture medium. Cells were prelabeled with green fluorescence (CellTrace CFSE Cell; Invitrogen) or red fluorescence (PKH26; Sigma-Aldrich), or were transduced with a GFP-lentivirus vector.[25] To block EphB/EphrinB interaction, cells were preincubated (1 hour) with SNEW plus TNYL-RAW or control peptides (100 μM) or with EphrinB2-Fc (10 μg/mL). The cells were photographed with a digital camera (Retiga 1300; Qimaging) under phase-contrast microscopy (1×51 with a 10×0.25 PhL lens; Olympus Optical); images obtained with IPLab for Windows software (Scanalytics) were imported into Adobe Photoshop. When immunostained with p-EphrinB antibody, cells on Matrigel were imaged with an Axiovert 200 fluorescence microscope (Carl Zeiss) using optimized excitation/emission filter sets (Omega Optical). Each label was captured through an appropriate filter set; images were digitized (OpenLab program; Improvision), and an appropriate color table was applied to match the emission spectrum or to set a distinguishing color balance. The pseudocolored images were converted into .tif files, exported to Adobe Photoshop (Adobe Systems), and overlaid as individual layers to create multicolored merged composites. For video microscopy, green fluorescent HUVEC and red fluorescent MSC (HUVEC, 4×10^4; BM-MSC, 2×10^4/chamber; complete HUVEC culture medium) were dispersed on Matrigel-coated LabTek chambers (Nalge Nunc International). Time-lapse microscopy[16] was carried out with an inverted confocal scanning microscope (LSM510 META; Carl Zeiss).

Mice

All animal experiments were approved by the National Cancer Institute Animal Care and Use Committee and conducted accordingly. C57BL/6J, BALB/cAnNcr, and nonobese diabetic (NOD)/severe combined immunodeficiency (SCID) mice were from The Jackson Laboratory.

Retinopathy of prematurity model

Newborn C57BL/6J mice and their nursing mothers were exposed to 75% oxygen from postnatal day (P)7 to P12 and then returned to room air.[27] To measure hypoxia, the mice were injected intraperitoneally with HypoxyProbe-1 (Chemicon Interational) 1 hour before sacrifice.

Wound healing

Excisional full-thickness wounds were made with 6-mm skin biopsy punches on the shaved backs of BALB/cAnNcr 6-week-old mice. Mice were killed on days 2 and 7 after wounding; the wounded areas were removed with adjacent normal skin and processed for histology.

Tumor model

The murine (BALB/c) MOPC315 plasmacytoma cell line (10×10^6 cells) was injected subcutaneously in the left abdominal quadrant of 6-week-old BALB/c mice. Tumors were removed after 2 weeks.

In vivo Matrigel assay

The assay was performed essentially as described.[28] Mice (female NOD/SCID and C57BL/6J, 6-7 weeks old) were injected subcutaneously with 0.5 mL of Matrigel (BD Biosciences) alone, Matrigel plus HUVEC (1.5×10^6 cells), Matrigel plus MSC (0.5×10^6 cells), Matrigel plus HUVEC (1.5×10^6 cells), plus MSC (0.5×10^6 cells). After 7 days, the Matrigel plugs were removed and processed for histology.

Statistical analysis

Results are expressed as means plus or minus SD. Student *t* test was used to evaluate group differences; a *P* value of less than .05 was considered significant.

Results

EphrinB is active in angiogenic blood vessels

The cytoplasmic domain of EphrinB ligands contains tyrosine residues that are phosphorylated in response to binding cognate EphB receptors or to fibroblast growth factor (FGF) receptor activation, initiating signaling referred to as reverse signaling.[6,29-32] Tyrosines 324/329 have been identified as major phosphorylation sites of EphrinB ligands.[31,32] To determine the phosphorylation status of EphrinB during postnatal vascular remodeling and thus establish when reverse signaling may be used, we used an antibody that specifically recognizes EphrinB when phosphorylated at tyrosines 324/329 (human, corresponding to tyrosines 323/328 in the mouse). At birth, no retinal vessels are present. Retinal vessels develop postnatally in the mouse.[33] By day 7 after birth (P7), vessels originating from the central retinal artery cover most of the surface of the retina; around P10, sprouting from the superficial retinal, vessels gives rise to the deep capillary bed. By P18, the adult retinal circulation is established and remains relatively stable thereafter.[33] We detected no EphrinB phosphorylation in adult mouse retinal vessels identified by immunostaining for the endothelial cell marker CD31 and the pericyte marker NG2[3] (Figure 1A), but confirmed[34] that these retinal vessels widely express EphrinB2 (supplemental Figure 1, available on the *Blood* website; see the Supplemental Materials link at the top of the online article). In contrast to adult retinas, we detected prominent EphrinB phosphorylation in the retinal vessels from P6 mice (Figure 1B and supplemental Figure 2). Much of the phosphorylated EphrinB localized to the CD31$^+$ endothelium and to a lower degree to NG2$^+$ pericytes. The close proximity of endothelial cells and pericytes often prevented a clear assignment of phosphorylated EphrinB to endothelial cells or pericytes, but selected images strongly suggested that EphrinB phosphorylation occurred in both cell types (Figure 1B). Immunoblotting detected progressively lower levels of phosphorylated EphrinB in mouse retinal lysates from P6, P13, and P15; virtually no phosphorylated EphrinB was detected by P17 (Figure 1C). These results show that EphrinB is phosphorylated in the developing retinal vasculature, but not in the adult retinal vasculature, suggesting that EphrinB activation marks angiogenic vessels.

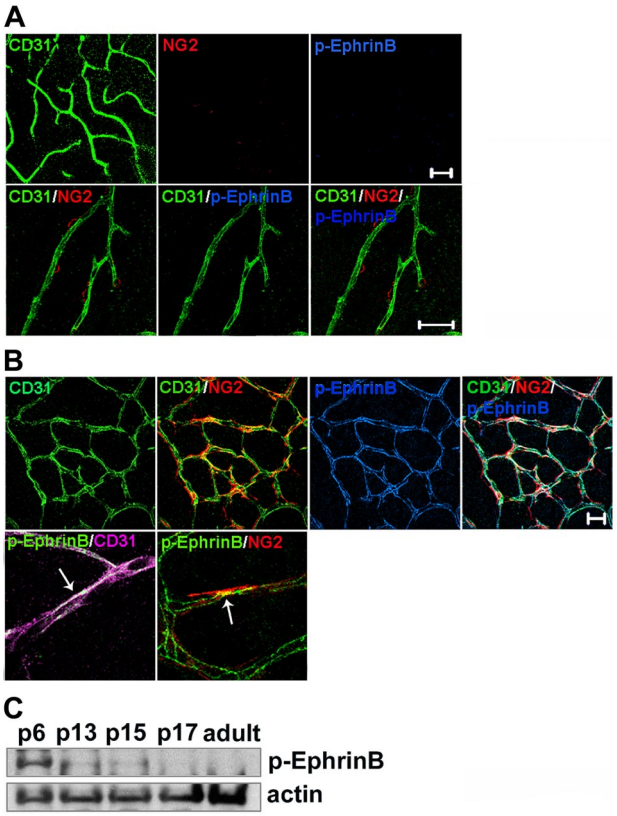

Figure 1. EphrinB is phosphorylated in developing, but not adult mouse retinal vessels. Retinal whole mounts from (A) adult (3-month-old) and (B) P6 mice were immunostained for CD31 (endothelial cells), NG2 (pericytes), and phospho (p)-EphrinB. Representative confocal images showing broad p-EphrinB detection in retinal vessels of P6, but not adult mice, overlapping with CD31 and partly NG2 immunostaining. Scale bars in panels A and B represent 20 μm. (C) p-EphrinB in retinal extracts from mice of different ages (from P6 to adult) detected by immunoblotting. The blot was stripped and reprobed for actin.

To test whether postnatal angiogenesis is more generally associated with EphrinB phosphorylation, we examined 3 distinct models of neovascularization: retinopathy of prematurity (ROP),[27] wound-induced skin neovascularization,[35] and tumor-associated neovascularization.[36] In the ROP model, 7-day-old mice are exposed to high (75%) oxygen tension for 5 days (P12), which stops retinal vascular development and promotes retinal vessel degeneration. This leads to retinal ischemia. Subsequent exposure of the mice to room air promotes retinal neovascularization. There were virtually no detectable $CD31^+$ vessels and little EphrinB phosphorylation in the hypoxic retinas from mice exposed to room air for only 1 day (P13), reflecting the expected vessel regression (Figure 2A). Instead, the retinal vessels that developed after 3-day exposure to room air (P15) displayed clear evidence of EphrinB phosphorylation (Figure 2A). After 5-day exposure to room air (P17), the retinal vasculature was further developed, but EphrinB phosphorylation was somewhat diminished (Figure 2A). This pattern of EphrinB activation in the regenerating retinal vessels was confirmed by immunoblotting the retinal extracts (Figure 2B).

In the skin wound-healing model,[35] we killed the mice 2 and 7 days after establishing full-thickness wounds. At the 2-day time point, we found that the edge of the wound was edematous and contained numerous $CD31^+$ cells with evidence of EphrinB phosphorylation (Figure 2C). EphrinB phosphorylation was also detected in some $CD31^-$ cells. Analysis of individual vessels from the wound margins revealed variable pericyte coverage, marked by NG2 immunostaining, and clear evidence of EphrinB phosphorylation in the $CD31^+$ endothelial cells and $NG2^+$ pericytes (Figure 2D). We found no evidence of EphrinB phosphorylation in vessels from the normal mouse skin and from wounded tissue removed from the mice after 7 days (Figure 2D and data not shown).

In the mouse tumor model, we injected subcutaneously the MOPC315 plasmacytoma cell line into syngeneic BALB/c mice.[36] The subcutaneous tumors that developed were highly vascular and the vessels were incompletely marked by $NG2^+$ pericytes (Figure 2E). EphrinB phosphorylation was confined to selected areas of the tumor vasculature, particularly where vessel density was greatest and pericytes were detected (Figure 2E). Thus, EphrinB is phosphorylated in angiogenic vessels from the retina, skin, and tumor tissues.

EphrinB activation in endothelial cells and bone marrow–derived MSC/pericytes

Our analysis suggested that EphrinB is activated in endothelial cells and pericytes during the angiogenic process in vivo. To confirm the occurrence of EphrinB activation in both cell types, we used human BM-MSC as a surrogate for primary cultures of pericytes because there is compelling evidence that such cells are phenotypically and functionally indistinguishable from MSC[3] and primary HUVEC as a source of endothelial cells.

By RT-PCR, MSC express EphrinB2 mRNA, but virtually no EphrinB1 and EphrinB3 (data not shown), and by immunoblotting MSC express EphrinB2 (Figure 3A). Previously, we established that HUVEC express EphrinB2 mRNA and protein, but not

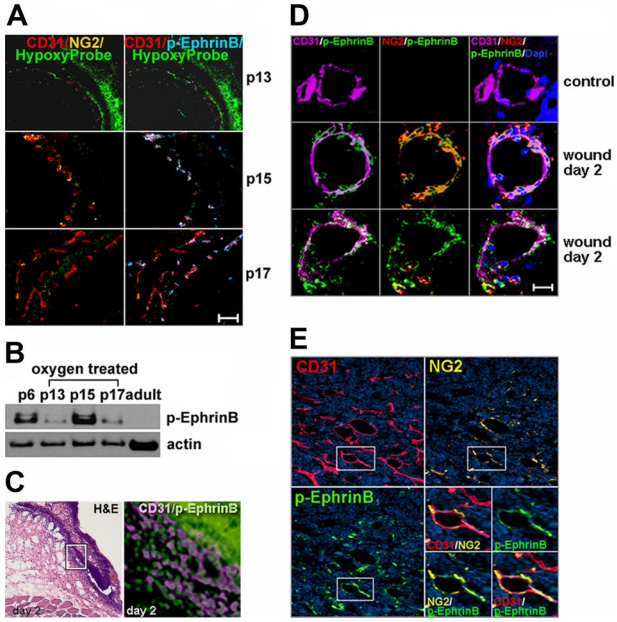

Figure 2. EphrinB phosphorylation marks angiogenic vessels. (A) ROP model: P7 mice were exposed to 75% oxygen tension for 5 days (P12) and then to normal oxygen tension for 1 day (P13), 3 days (P15), and 5 days (P17). Representative confocal images from retinal whole mounts show vascular p-EphrinB in p15 and p17. HypoxyProbe marks hypoxic areas. P13 original magnification ×10 p13 and ×20 p15 and p17. (B) p-EphrinB and actin in retinal extracts from p6, adult, and ROP (P13, P15, and P17) mice detected by immunoblotting. (C) Skin wound-healing model. Representative H&E staining (left) of a 2-day-old wound showing the disrupted epithelium; CD31 and p-EphrinB immunostaining of boxed area (expanded on the right). The epithelium displays intense nonspecific green fluorescence seen from secondary-only antibody. (D) Selected capillaries from control and wounded skin detected by confocal microscopy after immunostaining. (E) MOPC315 tumor model. Tumor vessels ($CD31^+$) show variable pericyte ($NG2^+$) coverage and p-EphrinB expression. The boxed area (expanded bottom right) shows vascular localization of p-EphrinB immunostaining. Scale bars in panels A and D represent 20 μm. Original magnification in panels C and E is ×20.

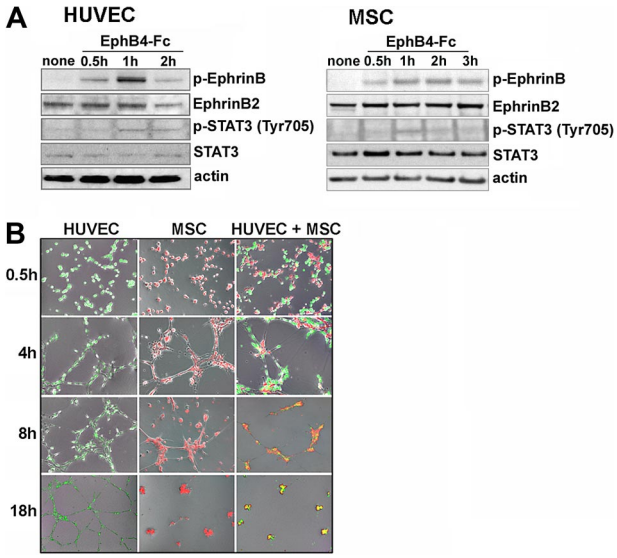

Figure 3. EphrinB phosphorylation and extracellular matrix-dependent cord formation by HUVEC and MSC. (A) Cell lysates from unstimulated or EphB4-Fc–stimulated HUVEC and MSC were immunoblotted with specific antibodies. (B) HUVEC marked by a green fluorescent dye (CellTrace CFSE) and MSC marked by a red fluorescent dye (PKH26) were incubated (37°C for 18 hours) individually or together (ratio 2:1) onto solidified Matrigel. Representative images from inverted fluorescence microscopy (original magnification ×4) showing time-dependent network formation.

EphrinB1 or EphrinB3.[16] Using recombinant EphB4-Fc to induce EphrinB2 phosphorylation,[37] we documented EphrinB phosphorylation in HUVEC and MSC, indicating that both cell types possess a functional cell surface EphrinB2 (Figure 3A). EphB4-Fc also induced phosphorylation of STAT3 in HUVEC and MSC (Figure 3A). STAT3 is a downstream effector of EphrinB activation.[31]

Because HUVEC and MSC express functional EphrinB2 ligands (Figure 3A) and the cognate EphB2 and EphB4 receptors (supplemental Figure 3), we examined whether cell-to-cell contact promotes EphrinB phosphorylation in these cells. When cultured at various cell densities on plastic either individually or mixed together, HUVEC and MSC display little EphrinB phosphorylation, indicating that cell-to-cell contact alone is insufficient for EphrinB activation in vitro (data not shown). We cultured HUVEC and MSC individually or together (at a ratio of 2:1 based on variable[38] pericyte coverage of the endothelium in different vascular beds) onto Matrigel, a mixture of extracellular matrix proteins, which promoted cord formation (Figure 3B). Under these conditions, EphrinB was time dependently activated in HUVEC and MSC when cultured individually (supplemental Figure 4A-D) or together (Figure 4A-B). The kinetics of EphrinB activation in this system were similar in both cell types when cultured individually or together: phosphorylation was generally detected at 1 and 2 hours when cordlike structures were actively forming, and was undetectable at 4 and 8 hours (Figure 4 and supplemental Figure 4A-D) and later (data not shown) time points. EphrinB phosphorylation was generally absent from isolated HUVEC and MSC that

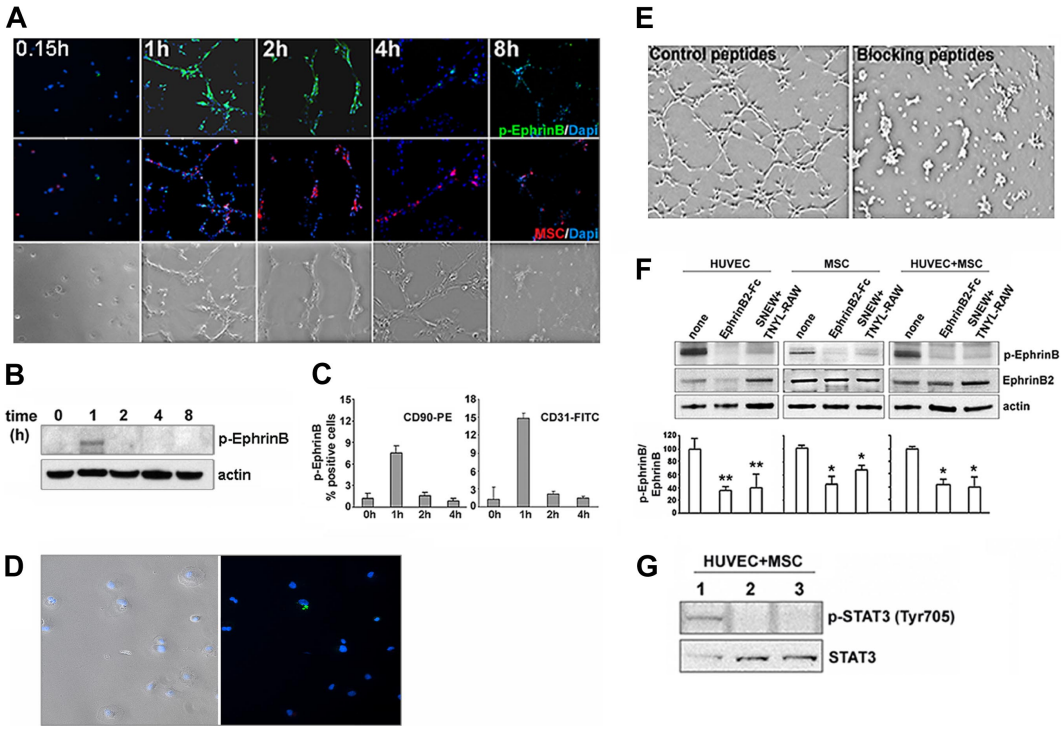

Figure 4. EphB-dependent activation of EphrinB in HUVEC and MSC incubated together on extracellular matrix. (A) Representative images showing p-EphrinB fluorescence immunostaining of HUVEC (unstained) and MSC (marked by red fluorescent dye PKH26red) cocultured on Matrigel. Bottom panels reflect images from bright-field microscopy. Original magnification ×20. (B) Time-dependent EphrinB activation in cocultures of HUVEC and MSC incubated on Matrigel detected by immunoblotting. (C) Flow cytometric detection of p-EphrinB in HUVEC ($CD31^+$) and MSC ($CD90^+$) removed from coculture on Matrigel at the indicated time points. The results reflect the means (± SD) of 3 independent experiments. (D) Representative images showing minimal p-EphrinB fluorescence in isolated cells from cocultures of HUVEC and MSC incubated 1 hour on Matrigel. Left panel: bright-field microscopy. Original magnification ×40. (E) Representative bright-field microscopy images from cocultures of HUVEC and MSC (ratio 2:1) incubated on Matrigel for 4 hours in the presence of the EphB receptor inhibitors SNEW and TNYL-RAW peptides. Original magnification ×4. (F) EphrinB2-Fc and peptides SNEW and TNYL-RAW reduce p-EphrinB in HUVEC and MSC incubated (2 hours) individually or together (ratio 2:1) on Matrigel. Representative immunoblotting results; the bar graph reflects the mean relative ratios (± SD) of p-EphrinB/total EphrinB2 band intensity detected by immunoblotting in 3 experiments. $^{**}P < .01$; $^{*}P < .05$. (G) p-STAT3 and STAT3 immunoblotting of cell lysates from HUVEC and MSC incubated (2 hours) together (ratio 2:1) on Matrigel in medium only (lane 1), with EphrinB2-Fc (lane 2), or with SNEW and TNYL-RAW peptides (lane 3). Results are from reprobing the membrane shown in panel E (right panel).

had failed to make contact with other cells (Figure 4D), suggesting that attachment to Matrigel alone does not promote EphrinB activation and requires instead cell-to-cell contact in this system.

The cordlike structures generated by HUVEC remained relatively stable more than 18 hours incubation on Matrigel, whereas those generated by MSC alone or with MSC characteristically disassembled and resolved into tight clusters after 8 to 18 hours' incubation (Figures 3B and 4A, supplemental Video 1). Such instability of Matrigel-supported vascular structures when mesenchymal cells are present was previously attributed to growth factor deficiency.[39] We found no evidence of EphrinB phosphorylation in MSC during this retraction phase (Figure 4A-B and supplemental Figure 4B-C).

In the Matrigel-supported cocultures, both HUVEC (unlabeled) and MSC (red) appeared to activate EphrinB during cord formation, as judged by immunofluorescence (Figure 4A). To confirm this observation, we examined separately MSC and HUVEC from the cocultures. By flow cytometry, we determined that EphrinB was phosphorylated in each of the cell populations ($CD90^+$ MSC and $CD31^+$ HUVEC) recovered from the cocultures, and confirmed the kinetics of EphrinB phosphorylation (Figure 4C). These experiments show that the active assembly of HUVEC and MSC into cordlike structures is temporally associated with activation of EphrinB in both cell types.

EphrinB phosphorylation identified at sites of pericyte/endothelial cell contact

To test whether EphrinB activation in Matrigel-supported cocultures is attributable to activation by cognate EphB receptors through cell-to-cell contact, we used specific blocking peptides[40] and soluble EphrinB2-Fc. A mixture of the SNEW (EphB2 inhibitor) and TNYL-RAW (EphB4 inhibitor) peptides blocked Matrigel-dependent cord formation by HUVEC and MSC cultured individually (data not shown) or mixed together (Figure 4E). In addition, the SNEW plus TNYL-RAW peptides and EphrinB2-Fc significantly reduced EphrinB phosphorylation (Figure 4F) and STAT3 phosphorylation (Figure 4G) in HUVEC and MSC cultured individually or together onto Matrigel.

Because both MSC and HUVEC express EphB2 and EphB4 receptors (Figure S3), the phosphorylation of EphrinB occurring in mixed cultures of HUVEC and MSC could arise from cell-to-cell interactions within each cell type or with each other. To test whether EphrinB phosphorylation occurs where HUVEC contact MSC, we used confocal microscopy-assisted imaging. We observed that extensions from MSC (red) make close contact and appear to push deep into HUVEC (green) when cocultured on Matrigel for 1 hour (Figure 5A). Importantly, EphrinB phosphorylation was evident at these contact points where MSC intimately contact HUVEC (Figure 5Ai-iv), providing evidence that cell-to-cell contact between MSC and HUVEC is associated with EphrinB phosphorylation in this system.

To confirm this observation, we used a mouse model of Matrigel-assisted vessel formation, in which Matrigel, GFP-MSC, and HUVEC are injected subcutaneously into immunodeficient mice. A week after injection, the HUVEC (identified by a human CD31-specific antibody) and the GFP-MSC gave rise to a vascular bed that anastomosed with the mouse vasculature as it contained red cell remnants/hemoglobin (detected by H&E as a red filling; Figure 5B). A mouse CD31-specific antibody (rat anti–mouse CD31; BD Pharmingen) visualized small vessels at the margins of the plug, but not the vascular structures marked by the human CD31-specific antibody (data not shown). The human cell–derived vascular bed was much reduced by the inclusion of 50 μM SNEW

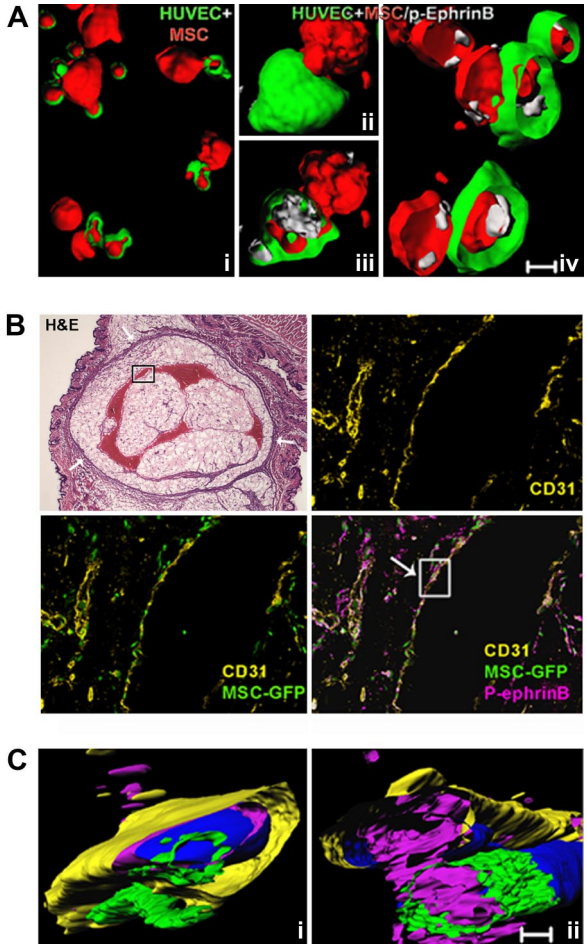

Figure 5. EphrinB is phosphorylated at sites of contact between endothelial cells and MSC. (A) Cell surface and interior rendering of representative confocal images showing MSC (red) contacting HUVEC (green), and p-EphrinB (white) at points of contact between HUVEC and MSC after 1-hour incubation on Matrigel. Subpanels iii and iv are the result of clipping to show the cell interior. (B) Representative microscopy images from H&E staining of a sectioned Matrigel plug (oval structure limited by a drawn black line), showing vessels containing remnants of red cells (red structures) and the overlying skin (original magnification ×1.2); and fluorescence immunostaining of human CD31 and p-EphrinB in sequential sections from the boxed area within the Matrigel plug containing HUVEC and GFP-MSC retrieved from the mouse after 7 days (original magnification ×20). (C) Three-dimensional rendering of confocal images from 2 segments of the boxed vessel wall in panel B showing the relationship between $CD31^+$ endothelium, GFP-labeled MSC, and p-EphrinB. Images reflect clipping and rotation to show relationships between cell types and p-EphrinB. Scale bars in panels A and C represent 50 μm.

and TNYL-RAW peptides in the Matrigel containing HUVEC and MSC (data not shown). In the absence of inhibitory peptides, GFP-labeled MSC and HUVEC (identified by human-specific CD31 antibodies) were visualized, both lining blood channels replete with erythrocytes and forming smaller vascular structures. EphrinB phosphorylation was evident along the larger vessel wall and in other sites where HUVEC and MSC were present. Analysis of reconstructed images from segments of the newly formed vessel wall identified phosphorylated EphrinB within HUVEC and MSC, where they come in contact with each other (Figure 5C and supplemental Video 2).

EphrinB2 is required for pericyte and endothelial cell assembly into cordlike structures

The occurrence of EphrinB phosphorylation during angiogenesis suggested that it mediates important roles. To test for this possibility, we silenced EphrinB2 expression by use of silencing RNA

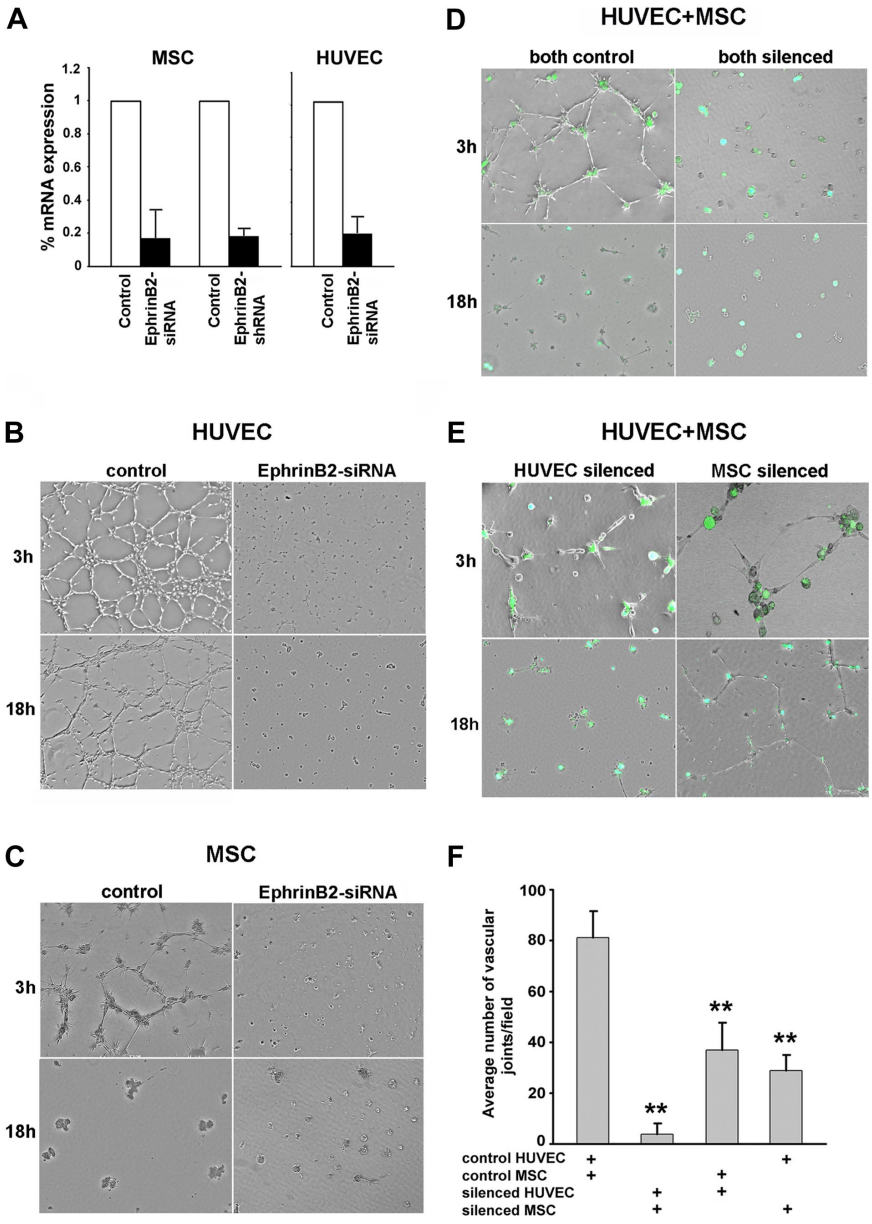

Figure 6. EphrinB2 silencing in HUVEC and MSC reduces cord formation. Reduction of EphrinB2 mRNA levels in HUVEC and MSC by silencing with siRNA or shRNA measured by real-time RT-PCR. The results reflect the means (± SD) of 3 independent experiments (A). Representative images from Matrigel-supported cultures of control and EphrinB2-silenced (siRNA) HUVEC (B), control and EphrinB2-silenced MSC (siRNA) (C), cocultures of HUVEC and MSC (both silenced: HUVEC by siRNA, MSC by GFP-shRNA) (D), and cocultures of HUVEC and MSC in which HUVEC or MSC was silenced (E). Network formation in Matrigel-supported cocultures of HUVEC (control or siRNA) and MSC (control or shRNA) was measured as the mean number of angles (± SD) generated by intersecting cords from 3 separate experiments; ** $P < .01$ (F).

duplexes (siRNA) or a lentivirus vector expressing shRNA. We achieved a marked reduction of EphrinB2 mRNA levels in MSC and HUVEC by one or both methods, without compromising cell viability (Figure 6A). The silencing of EphrinB2 expression in HUVEC and MSC prevented formation of cordlike structures when HUVEC and MSC were incubated individually (Figure 6B-C) or together (Figure 6D) on Matrigel. When EphrinB2 was silenced in HUVEC or in MSC and the cells were then mixed with nonsilenced MSC or HUVEC, respectively (Figure 6E), cord formation was impaired during the initial 4-hour observation (3-hour time point is shown; Figure 6F). However, the late (18-hour time point) clustering of HUVEC and MSC occurred normally when EphrinB2 was silenced in the HUVEC (Figure 6E left), but not when EphrinB2 was silenced in the MSC; in this study, the cordlike structures that had formed, albeit reduced in number, appeared relatively stable (Figure 6E right). We conclude that both HUVEC and MSC must express EphrinB to optimally assemble with each other in cordlike structures. When EphrinB was silenced, HUVEC and MSC formed clumps, rather than cords, on Matrigel (Figure 6D), and failed to display p-EphrinB at contact points (data not shown). The results further suggest that the late cord retraction in Matrigel cultures, which is driven by MSC, requires MSC expression of EphrinB2. Because we observe no EphrinB phosphorylation in retracting cocultures (Figure 4A-B and supplemental Figure 4B-C), this function of EphrinB2 appears independent of EphrinB phosphorylation.

These experiments demonstrated that EphrinB expression is required for proper assembly of HUVEC and MSC on extracellular matrix, but could not distinguish between the dual role of EphrinB as a reverse signaling molecule and a ligand for EphB activation. We focused on EphrinB phosphorylation within the cytoplasmic domain, which initiates EphrinB reverse signaling.[6,29-32,41] A tyrosine phosphorylation-deficient EYFP-EphrinB2 mutant (EphrinB2^{5F}, in which all 5 conserved tyrosines are substituted by phenylalanine) or wild-type EYFP-EphrinB2^{WT} was transduced into HUVEC and MSC. Viability was somewhat compromised in the EYFP-EphrinB2^{5F}-transfected HUVEC and to a lower degree in MSC. Unlike HUVEC and MSC transduced

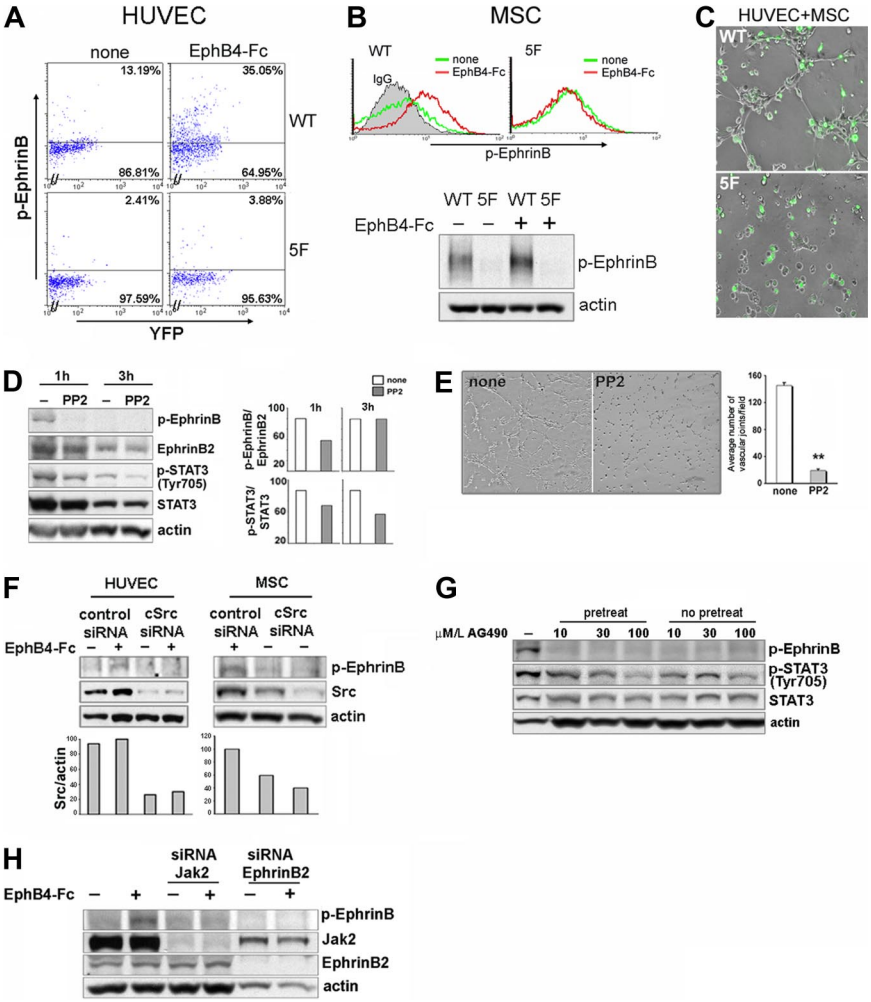

Figure 7. Contribution of EphrinB signaling to extracellular matrix-dependent assembly of HUVEC and MSC. (A-B) Flow cytometric detection of p-EphrinB in HUVEC and MSC transduced with wild-type EYFP-EphrinB2^{WT} (WT) or mutant EYFP-EphrimB2^{5F} (5F), with or without stimulation with EphB4-Fc (45 minutes). (B) Bottom reflects p-EphrinB and actin immunoblotting of MSC transduced with EYFP-EphrinB2^{WT} or mutant EYFP-EphrimB2^{5F} after sorting for YFP (> 90%) and stimulation with or without EphB4-Fc (45 minutes). (C) Matrigel-dependent cord formation by cocultures of YFP-sorted HUVEC and MSC transduced with EYFP-EphrinB2^{WT} (WT) or mutant EYFP-EphrimB2^{5F} (5F). WT reflects coculture of HUVEC and MSC transduced with EYFP-EphrinB2^{WT} (WT); 5F reflects coculture of HUVEC and MSC transduced with mutant EYFP-EphrimB2^{5F} (5F). (D) Western blot analysis of p-EphrinB and p-STAT3 expression in cocultures of HUVEC and MSC (ratio 2:1) incubated 1 and 3 hours in medium only or with PP2 onto Matrigel. The bar graph reflects relative ratios of p-EphrinB/EphrinB and p-STAT3/STAT3. (E) Representative images reflecting cord formation by HUVEC and MSC cocultured (ratio 2:1) on Matrigel for 1.5 hours. The bar graph reflects measurement of Matrigel-dependent network formation by HUVEC and MSC cultured together with or without PP2, as reflected by mean number of angles (± SD) generated by intersecting cords from 3 separate experiments; $^{**}P < .01$. (F) Src silencing reduces EphB4-induced p-EphrinB in HUVEC and MSC. Western blot analysis of total Src and p-EphrinB in control (Risc-free siRNA) and Src-silenced HUVEC and MSC, with or without EphB4-Fc activation. The bar graph reflects relative ratios of Src/actin. (G) Effects of AG490 on p-EphrinB and p-STAT3 expression in cocultures of HUVEC and MSC (ratio 2:1) incubated onto Matrigel. Cells were incubated with AG490 on Matrigel with or without AG490 pretreatment (1-hour incubation with AG490). Results reflect immunoblotting with specific antibodies. (H) Jak2 silencing reduces EphB4-induced p-EphrinB in HUVEC. Western blot analysis of p-EphrinB, Jak2, EphrinB2, and actin in control (Risc-free siRNA), Jak2, or EphrinB2-silenced HUVEC, with or without EphB4 activation.

with EYFP-EphrinB2^{WT} (WT), the EYFP-positive viable HUVEC and MSC transduced with EYFP-EphrinB2^{5F} (5F) displayed minimal EphB4-induced EphrinB phosphorylation (Figure 7A-B). When cultured together on Matrigel, EYPP-EphrinB2^{5F} mutant HUVEC and MSC displayed a significantly reduced ability to assemble into cordlike structures compared with control cells transduced with EYFP-EphrinB2^{WT} (Figure 7C), providing evidence that EphrinB2 reverse signaling is critical to endothelial/pericyte assembly in this system.

Because Src family kinases are responsible for EphB-induced phosphorylation of EphrinB,[5,42] we examined the effects of Src kinase inhibition. We found that 10 μM PP2, a specific inhibitor of the Src family kinases, reduced EphrinB phosphorylation induced by cell-to-cell contact in HUVEC and MSC incubated onto Matrigel (Figure 7D). PP2 also inhibited STAT3 phosphorylation (Figure 7D), a downstream effector of EphrinB phosphorylation.[31] When present continuously during culture, PP2 reduced Matrigel-dependent cord formation by mixtures of HUVEC and MSC (Figure 7E). We also silenced Src expression in HUVEC and MSC by siRNA. In contrast to control cells, Src-deficient MSC and HUVEC failed to activate EphrinB phosphorylation in the presence of EphB4-Fc (Figure 7F), and failed to assemble into cordlike structures when incubated individually (supplemental Figure 5) together on Matrigel (data not shown). Thus, Src activation is required for EphrinB phosphorylation and assembly of HUVEC and MSC on extracellular matrix.

To further address the role of EphrinB reverse signaling, we took advantage of the observation that STAT3 activation induced by phosphorylated EphrinB is Jak2 dependent.[31] We found that Tyrphostin AG490, a Jak2 inhibitor,[43] dose dependently reduced EphrinB and STAT3 phosphorylation detected in cocultures of HUVEC and MSC incubated on Matrigel (Figure 7G), and impaired cord formation by HUVEC and MSC comparably to PP2 (data not shown). We also silenced Jak2 expression in HUVEC by siRNA. Unlike control cells, Jak2-deficient HUVEC displayed little EphrinB2 activation with EphB4-Fc, similar to EphrinB2-silenced HUVEC (Figure 7H). Together, these observations provide evidence for a contribution of EphrinB reverse signaling in the extracellular matrix–mediated assembly of endothelial cells and pericytes.

Discussion

Neovascularization requires that endothelial cells and pericytes proliferate, migrate to the proper location, and assemble into vascular structures. In this study, we show that EphrinB2, a transmembrane ligand for EphB receptors, is a critical mediator of endothelial-to-pericyte assembly during postnatal vascular remodeling. This function requires cell-to-cell contact, leading to EphrinB2 engagement by EphB surface-bound receptors, and is

dependent upon tyrosine phosphorylation of EphrinB2 intracellular domain.

Previous studies of mutant mice have demonstrated that vascular ephrinB2 and its cognate EphB receptors play critical functions in vascular development. In particular, the total knockout of EphrinB2, the endothelium-specific knockout of EphrinB2, or the deletion of the cytoplasmic domain of EphrinB2 causes similar defects in the remodeling of the primary capillary plexus.[8-10,13,44] The devastating developmental consequences of deletion of EphrinB2 intracellular domain established the importance of EphrinB2 intracellular domain in the developing vessels, and suggested that the role of EphrinB2 is not limited to its ability to activate EphB receptors. Supporting this possibility, chimeric mice harboring a mutation in the EphrinB1 PDZ domain were generally nonviable and displayed abnormalities in neural crest cell-derived tissues.[45] However, knock-in mice expressing EphrinB2 in which the conserved tyrosine residues in the intracytoplasmic domain were replaced with phenylalanine to disrupt phosphotyrosine-dependent signaling or lacking the C-terminal PDZ interaction site had no appreciable vascular defects,[12] raising unresolved questions on the contribution of EphrinB signaling to vascular development.

Previous experiments are clear in documenting the occurrence of tyrosine phosphorylation within the C-terminal domain of EphrinB. In vitro, cell-associated EphrinB binding to a cognate EphB receptor,[5,6] engagement of the tight junction protein claudin,[46] and activation of the FGF receptor[47] can induce EphrinB1 phosphorylation. In vivo, EphrinB phosphorylation is noted in mouse embryo extracts,[6] in the developing chicken retina,[32] and in the vasculature of tumor xenografts, where the tumor cells were transduced with EphB4.[30] In this study, we show that EphB4-Fc induces EphrinB phosphorylation in primary endothelial cells and in bone marrow-derived MSC/pericytes. We also show that EphrinB is prominently phosphorylated in endothelial cells and pericytes within the developing vessels of the mouse retina and in the remodeling vasculature of wounded skin and in tumor tissue. Thus, EphrinB phosphorylation marks angiogenic vessels.

Hypoxia and vascular endothelial growth factor, which serve as principal endogenous stimulators of physiologic and pathologic angiogenesis and most likely contributed to angiogenesis in the model systems investigated in this study, can promote endothelial cell expression of EphrinB2, but not its phosphorylation.[48] Despite previous studies suggesting that there may be some level of EphB/EphrinB signaling even in the absence of cell-to-cell contact,[13] our experiments show that EphrinB requires engagement by EphB receptors through cell-to-cell contact for activation and reverse signaling. Several lines of evidence support this conclusion. First, there is a temporal association between the occurrence of cell-to-cell contact and the activation of EphrinB. Second, we find that EphrinB is phosphorylated at the precise cell-to-cell contact points. Third, specific blockers of EphB/EphrinB engagement prevent EphrinB activation in endothelial cells and pericytes.

One of the important findings in our studies is the critical contribution of extracellular matrix to EphrinB phosphorylation in cell-to-cell interactions of endothelial cells and pericytes. Although not surprising in view of the intimate contact that exists between endothelium, pericytes, and basement membrane (which is composed of extracellular matrix proteins), this leads to the question of how Eph/Ephrin molecules and extracellular matrix proteins are linked. We suspect that this link comes from cross-talk between Eph/Ephrin signaling and other signaling pathways.[29] Previous studies have demonstrated cooperation between the stromal cell–derived factor-1/CXCR4 and EphB/EphrinB signaling cascades in human and mouse cells,[16,41] and between the extracellular matrix protein fibronectin and its receptor integrin α_5 with the Eph/Ephrin system in the developing zebrafish.[49]

In agreement with genetic studies showing important contributions of EphrinB intracellular domain to vascular and neuronal development,[10,45] we show in this study that blockade of Src or Jak2 kinase activity impairs endothelial/pericyte assembly on extracellular matrix, providing evidence for the critical importance of ephrinB reverse signaling in mediating in the assembly of endothelial cells and pericytes. Several studies of EphrinB reverse signaling have concluded that Src family kinases are critical contributors of EphrinB phosphorylation.[5,6,42] More recently, Jak2-dependent STAT3 activation was identified a downstream mediator of EphrinB signaling.[31] The mechanisms by which EphrinB reverse signaling contributes to endothelial cells-to-pericytes assembly require further investigation, but may involve a contribution by the adaptor protein growth factor receptor-bound protein 4, which binds the cytoplasmic domain of phosphorylated EphrinB increasing focal adhesion kinase catalytic activity, leading to a redistribution of paxillin and disassembly of F-actin-containing stress fibers.[50] It is unlikely that STAT3 contributes to endothelial/pericyte assembly by regulating gene transcription because critical events occurred within the first 1-4 hours, sooner than expected from a transcriptional effect of STAT3. However, besides its activity as a nuclear transcriptional activator, STAT3 was reported to regulate microtule stability by interacting with the tubulin-depolymerizing protein stathmin.[51]

Various approaches to interference of EphB/ephrinB binding have resulted in inhibition of tumor growth in some mouse tumor models, but promoted tumor angiogenesis and tumor growth in other models.[52] The critical importance of EphrinB reverse signaling in the assembly of endothelial cells and pericytes emerging from the current studies raises the possibility that selective targeting EphrinB reverse signaling may represent a novel approach to destabilizing the vessel wall to inhibit tumor angiogenesis.

Acknowledgments

We thank Susan Garfield for confocal microscopy imaging; Lucy Sierra for technical support; and Drs Ira Daar, Triantafyllos Chavakis, Peter McCormick, Marta Segarra, Paola Gasperini, Stuart H. Yuspa, and Doug Lowy for their help on various aspects of this work.

This work was supported by the Intramural Research Program of the National Institutes of Health, National Cancer Institute, Center for Cancer Research.

Authorship

Contribution: O.S. and G.T. designed research, analyzed data, and wrote the paper; D.M., M.E., and S.S. performed some experiments; and S.M. and A.F. generated critical reagents.

Conflict-of-interest disclosure: The authors declare no competing financial interests.

Correspondence: Ombretta Salvucci, 37 Covent Dr, Rm 4134, Laboratory of Cellular Oncology, Center for Cancer Research, National Cancer Institute, National Institutes of Health, Bethesda, MD 20892; e-mail: salvucco@mail.nih.gov.

References

1. Cuevas P, Gutierrez-Diaz JA, Reimers D, Dujovny M, Diaz FG, Ausman JI. Pericyte endothelial gap junctions in human cerebral capillaries. *Anat Embryol*. 1984;170:155-159.
2. Armulik A, Abramsson A, Betsholtz C. Endothelial/Pericyte interactions. *Circ Res*. 2005;97:512-523.
3. Crisan M, Yap S, Casteilla L, et al. A perivascular origin for mesenchymal stem cells in multiple human organs. *Cell Stem Cell*. 2008;3:301-313.
4. Kuijper S, Turner CJ, Adams RH. Regulation of angiogenesis by Eph-ephrin interactions. *Trends Cardiovasc Med*. 2007;17:145-151.
5. Bruckner K, Pasquale EB, Klein R. Tyrosine phosphorylation of transmembrane ligands for Eph receptors. *Science*. 1997;275:1640-1643.
6. Holland SJ, Gale NW, Mbamalu G, Yancopoulos GD, Henkemeyer M, Pawson T. Bidirectional signalling through the EPH-family receptor Nuk and its transmembrane ligands. *Nature*. 1996;383:722-725.
7. Adams RH, Wilkinson GA, Weiss C, et al. Roles of ephrinB ligands and EphB receptors in cardiovascular development: demarcation of arterial/venous domains, vascular morphogenesis, and sprouting angiogenesis. *Genes Dev*. 1999;13:295-306.
8. Gerety SS, Wang HU, Chen ZF, Anderson DJ. Symmetrical mutant phenotypes of the receptor EphB4 and its specific transmembrane ligand ephrin-B2 in cardiovascular development. *Mol Cell*. 1999;4:403-414.
9. Gerety SS, Anderson DJ. Cardiovascular ephrinB2 function is essential for embryonic angiogenesis. *Development*. 2002;129:1397-1410.
10. Adams RH, Diella F, Hennig S, Helmbacher F, Deutsch U, Klein R. The cytoplasmic domain of the ligand ephrinB2 is required for vascular morphogenesis but not cranial neural crest migration. *Cell*. 2001;104:57-69.
11. Cowan CA, Yokoyama N, Saxena A, et al. Ephrin-B2 reverse signaling is required for axon path finding and cardiac valve formation but not early vascular development. *Dev Biol*. 2004;271:263-271.
12. Makinen T, Adams RH, Bailey J, et al. PDZ interaction site in ephrinB2 is required for the remodeling of lymphatic vasculature. *Genes Dev*. 2005;19:397-410.
13. Foo SS, Turner CJ, Adams S, et al. Ephrin-B2 controls cell motility and adhesion during blood-vessel-wall assembly. *Cell*. 2006;124:161-173.
14. Gale NW, Baluk P, Pan L, et al. Ephrin-B2 selectively marks arterial vessels and neovascularization sites in the adult, with expression in both endothelial and smooth-muscle cells. *Dev Biol*. 2001;230:151-160.
15. Shin D, Garcia-Cardena G, Hayashi S, et al. Expression of ephrinB2 identifies a stable genetic difference between arterial and venous vascular smooth muscle as well as endothelial cells, and marks subsets of microvessels at sites of adult neovascularization. *Dev Biol*. 2001;230:139-150.
16. Salvucci O, de la Luz Sierra M, Martina JA, McCormick PJ, Tosato G. EphB2 and EphB4 receptors forward signaling promotes SDF-1-induced endothelial cell chemotaxis and branching remodeling. *Blood*. 2006;108:2914-2922.
17. Korff T, Braun J, Pfaff D, Augustin HG, Hecker M. Role of ephrinB2 expression in endothelial cells during arteriogenesis: impact on smooth muscle cell migration and monocyte recruitment. *Blood*. 2008;112:73-81.
18. Huynh-Do U, Vindis C, Liu H, et al. Ephrin-B1 transduces signals to activate integrin-mediated migration, attachment and angiogenesis. *J Cell Sci*. 2002;115:3073-3081.
19. Maekawa H, Oike Y, Kanda S, et al. Ephrin-B2 induces migration of endothelial cells through the phosphatidylinositol-3 kinase pathway and promotes angiogenesis in adult vasculature. *Arterioscler Thromb Vasc Biol*. 2003;23:2008-2014.
20. Steinle JJ, Meininger CJ, Forough R, Wu G, Wu MH, Granger HJ. Eph B4 receptor signaling mediates endothelial cell migration and proliferation via the phosphatidylinositol 3-kinase pathway. *J Biol Chem*. 2002;277:43830-43835.
21. Fuller T, Korff T, Kilian A, Dandekar G, Augustin HG. Forward EphB4 signaling in endothelial cells controls cellular repulsion and segregation from ephrinB2 positive cells. *J Cell Sci*. 2003;116:2461-2470.
22. Kim I, Ryu YS, Kwak HJ, et al. EphB ligand, ephrinB2, suppresses the VEGF- and angiopoietin 1-induced Ras/mitogen-activated protein kinase pathway in venous endothelial cells. *FASEB J*. 2002;16:1126-1128.
23. Salvucci O, Yao L, Villalba S, Sajewicz A, Pittaluga S, Tosato G. Regulation of endothelial cell branching morphogenesis by endogenous chemokine stromal-derived factor-1. *Blood*. 2002;99:2703-2711.
24. Follenzi A, Naldini L. Generation of HIV-1 derived lentiviral vectors. *Methods Enzymol*. 2002;346:454-465.
25. Follenzi A, Ailles LE, Bakovic S, Geuna M, Naldini L. Gene transfer by lentiviral vectors is limited by nuclear translocation and rescued by HIV-1 pol sequences. *Nat Genet*. 2000;25:217-222.
26. Yao L, Salvucci O, Cardones AR, et al. Selective expression of stromal-derived factor-1 in the capillary vascular endothelium plays a role in Kaposi sarcoma pathogenesis. *Blood*. 2003;102:3900-3905.
27. Smith LE, Wesolowski E, McLellan A, et al. Oxygen-induced retinopathy in the mouse. *Invest Ophthalmol Vis Sci*. 1994;35:101-111.
28. Angiolillo AL, Sgadari C, Taub DD, et al. Human interferon-inducible protein 10 is a potent inhibitor of angiogenesis in vivo. *J Exp Med*. 1995;182:155-162.
29. Arvanitis D, Davy A. Eph/Ephrin signaling: networks. *Genes Dev*. 2008;22:416-429.
30. Erber R, Eichelsbacher U, Powajbo V, et al. EphB4 controls blood vascular morphogenesis during postnatal angiogenesis. *EMBO J*. 2006;25:628-641.
31. Bong YS, Lee HS, Carim-Todd L, et al. EphrinB1 signals from the cell surface to the nucleus by recruitment of STAT3. *Proc Natl Acad Sci U S A*. 2007;104:17305-17310.
32. Kalo MS, Yu HH, Pasquale EB. In vivo tyrosine phosphorylation sites of activated ephrin-B1 and ephB2 from neural tissue. *Biol Chem*. 2001;276:38940-38948.
33. Campochiaro PA, Hackett SF. Ocular neovascularization: a valuable model system. *Oncogene*. 2003;22:6537-6548.
34. Zamora DO, Davies MH, Planck SR, Rosenbaum JT, Powers MR. Soluble forms of EphrinB2 and EphB4 reduce retinal neovascularization in a model of proliferative retinopathy. *Invest Ophthalmol Vis Sci*. 2005;46:2175-2182.
35. Echtermeyer F, Streit M, Wilcox-Adelman S, et al. Delayed wound repair and impaired angiogenesis in mice lacking syndecan-4. *J Clin Invest*. 2001;107:R9-R14.
36. Segarra M, Williams CK, Sierra Mde L, et al. Dll4 activation of Notch signaling reduces tumor vascularity and inhibits tumor growth. *Blood*. 2008;112:1904-1911.
37. Pasquale EB. Eph-Ephrin promiscuity is now crystal clear. *Nat Neurosci*. 2004;7:417-418.
38. Shepro D, Morel NM. Pericyte physiology. *FASEB J*. 1993;7:1031-1038.
39. Bryan BA, D'Amore PA. Pericyte isolation and use in endothelial/pericyte coculture models. *Methods Enzymol*. 2008;443:315-331.
40. Koolpe M, Burgess R, Dail M, Pasquale EB. EphB receptor-binding peptides identified by phage display enable design of an antagonist with ephrin-like affinity. *J Biol Chem*. 2005;280:17301-17311.
41. Lu Q, Sun EE, Klein RS, Flanagan JG. Ephrin-B reverse signaling is mediated by a novel PDZ-RGS protein and selectively inhibits G protein-coupled chemoattraction. *Cell*. 2001;105:69-79.
42. Palmer A, Zimmer M, Erdmann KS, et al. EphrinB phosphorylation and reverse signaling: regulation by Src kinases and PTP-BL phosphatase. *Mol Cell*. 2002;9:725-737.
43. Catlett-Falcone R, Dalton WS, Jove R. STAT proteins as novel targets for cancer therapy: signal transducer an activator of transcription. *Curr Opin Oncol*. 1999;11:490-496.
44. Wang HU, Chen ZF, Anderson DJ. Molecular distinction and angiogenic interaction between embryonic arteries and veins revealed by ephrin-B2 and its receptor Eph-B4. *Cell*. 1998;93:741-753.
45. Davy A, Aubin J, Soriano P. Ephrin-B1 forward and reverse signaling are required during mouse development. *Genes Dev*. 2004;18:572-583.
46. Tanaka M, Kamata R, Sakai R. Phosphorylation of ephrin-B1 via the interaction with claudin following cell-cell contact formation. *EMBO J*. 2005;24:3700-3711.
47. Chong LD, Park EK, Latimer E, Friesel R, Daar IO. Fibroblast growth factor receptor-mediated rescue of x-ephrin B1-induced cell dissociation in *Xenopus* embryos. *Mol Cell Biol*. 2000;20:724-734.
48. Pasquale EB. Eph-Ephrin bidirectional signaling in physiology and disease. *Cell*. 2008;133:38-52.
49. Koshida S, Kishimoto Y, Ustumi H, et al. Integrin α_5-dependent fibronectin accumulation for maintenance of somite boundaries in zebrafish embryos. *Dev Cell*. 2005;8:587-598.
50. Cowan CA, Henkemeyer M. The SH2/SH3 adaptor Grb4 transduces B-ephrin reverse signals. *Nature*. 2001;413:174-179.
51. Ng DC, Lin BH, Lim CP, et al. Stat3 regulates microtubules by antagonizing the depolymerization activity of stathmin. *J Cell Biol*. 2006;172:245-257.
52. Noren NK, Pasquale EB. Paradoxes of the EphB4 receptor in cancer. *Cancer Res*. 2007;67:3994-3997.